



Contents lists available at ScienceDirect

Arabian Journal of Chemistry

journal homepage: www.ksu.edu.sa

Original article



Exploring the mechanism of *Semen Cuscutae* processed with salt solution in improving kidney deficiency miscarriage based on serum pharmacology and network pharmacology

Xue Zhang^{a,1}, Yu Huang^{a,1}, Zhitong Yang^{a,1}, Baiyang Xu^a, Zilu Liu^a, Ximeng Ding^a, Qiumei Zhou^d, Gang Cao^e, Weidong Li^f, Chuanshan Jin^{a,b,c}, Shanshan Li^g, Xiaoli Wang^{a,b,c,*}, Jijun Chu^{h,*}

^a Anhui Province Key Laboratory of Research & Development of Chinese Medicine, Anhui University of Chinese Medicine, Hefei 230012, China

^b Heritage Base of TCM Processing Technology of NATCM, Anhui University of Chinese Medicine, Hefei 230012, China

^c Anhui Province Key Laboratory of Traditional Chinese Medicine Decoction Pieces of New Manufacturing Technology, Bozhou 236800, China

^d The First Affiliated Hospital of Anhui University of Chinese Medicine, Hefei 230031, China

^e School of Pharmacy, Zhejiang Chinese Medical University, Hangzhou 310053, China

^f School of Pharmacy, Nanjing University of Chinese Medicine, Nanjing 210023, China

^g School of Pharmacy, Bengbu Medical College, Bengbu 233000, China

^h Department of Reproductive Medicine, The First Affiliated Hospital of Anhui University of Chinese Medicine, Hefei 230031, China

ARTICLE INFO

Keywords:

Semen Cuscutae processed with salt solution
UHPLC-Q/TOF-MS
Kidney Deficiency Miscarriage
Network pharmacology

ABSTRACT

Semen Cuscutae (S) is an effective traditional Chinese medicine (TCM) in clinical practice for tonifying the kidney and calming the fetus. The effects of S on benefiting the kidney, fixing essence and calming the fetus were enhanced after salt processed. However, its bioactive substance and relevant mechanism have not been clearly yet. This study aims to explore the effective components of *Semen Cuscutae* processed with salt solution (Y) and its potential mechanism on the treatment of kidney deficiency miscarriage (KDM) with multi-components and multi-targets. In this study, serum pharmacology and network pharmacology were used to investigate the active ingredients and molecular mechanism of Y in improving kidney deficiency miscarriage. A rat model of kidney deficiency miscarriage was established using hydroxyurea combine with mifepristone to assess the effect of S on tonifying the kidney and calming the fetus. The results show that 13 active ingredients derived from Y were identified by serum pharmacology analysis. 92 common targets of active ingredients of Y and diseases were screened by network pharmacology, including 18 key targets (TP53, AKT1, TNF, IL6, VEGFA, CASP3, JUN, EGFR, etc). The KEGG pathway enrichment analysis showed that it was mainly concentrated in PI3K/Akt signaling pathway, and it was speculated that Y may protect pregnancy through PI3K/AKT and other signaling pathways with multi-component, multi-target and multi-pathway action characteristics. Animal pharmacodynamic analysis suggested that Y showed the better effect on the hydroxyurea combine with mifepristone induced abortion compared to the raw products of S. This study laid the foundation to identify the active components and potential mechanisms of Y in improving KDM by combining the in-tegrated methods of serum pharmacology and network pharmacology.

Abbreviations: S, raw products of *Semen Cuscuta*; Y, *Semen Cuscutae* processed with salt solution; KDM, kidney deficiency miscarriage; GO, gene ontology; KEGG, kyoto encyclopedia of genes and genomes; PPI, protein-protein interaction; UB, uterine bleeding; ELR, embryo loss rate; ELISA, enzyme-linked immunosorbent assay; HE, hematoxylin-eosin staining; OPLS-DA, the orthogonal partial least squares discriminate analysis; PCA, principal component analysis; VEGF, vascular endothelial growth factor; OD, optical density; IOD, integrated optical density.

Peer review under responsibility of King Saud University.

* Corresponding authors at: College of Pharmacy, Anhui University of Chinese Medicine, Hefei 230012(X. Wang), The First Affiliated Hospital of Anhui University of Chinese Medicine, Hefei 230031(J. Chu).

E-mail addresses: 792511843@qq.com (X. Wang), chujijun88888@163.com (J. Chu).

¹ Authors contributed equally to this work and shared co-first authorship.

<https://doi.org/10.1016/j.arabjc.2023.105456>

Received 14 July 2023; Accepted 12 November 2023

Available online 13 November 2023

1878-5352/© 2023 The Authors. Published by Elsevier B.V. on behalf of King Saud University. This is an open access article under the CC BY-NC-ND license (<http://creativecommons.org/licenses/by-nc-nd/4.0/>).

1. Introduction

Miscarriage, defined as spontaneous abortion before 20 weeks of gestation, is a common complication encountered during pregnancy, with a prevalence of about 20 % (Avant 1983, Wahabi et al., 2018). In the TCM theories, miscarriage belongs to the “category of fetal leakage” and “fetal movement”. Moreover, TCM has the concept of “the kidney storing essence and governing reproduction” and “if the kidney is full of qi, there will be a child”, suggesting that the fetal movement and miscarriage are mostly related to the lack of kidney essence and kidney qi. Kidney Qi, kidney essence and kidney Yang respectively maintain fetal safe, nourishing and warm (HUANG and CHEN, 2021). Therefore, tonifying the kidney and consolidating the essence are important treatment for kidney deficiency miscarriage (KDM). Recent years, evidence increasingly shows that a good vascular network and adequate blood flow at the maternal-fetal interface is an important factor for a successful pregnancy (Tan et al., 2015, Kaczynski et al., 2020). The maternal-fetal interface is the meconium, the peripheral blood vessels of which is called “cytosolic veins” in Chinese medicine. “Suwen Qibing Lun” record that “the collaterals of the uterus connecting with the kidney”, which clearly shows that the cytosol is an important pathway for the kidney essence and kidney qi to be infused into the fetal womb to nourish the fetus. In summary, sufficient kidney essence and kidney qi attached to the cellular vein, provide certain benefits to the fetus. The previous research of this group based on clinical data showed that *Semen Cuscutae* processed with salt solution processed with salt solution (Y) ranked first in the frequency of drug use for the treatment of KDM (Supplementary Figs. 1-2 and Supplementary Table 1).

Semen cuscutae (S), as well-known Chinese medicine, was first recorded in the “*Shen Nong's Herbal*”, belongs to *Cuscuta australis* R. Br. or *Cuscuta chinensis* Lam. of Convolvulaceae family. It has the effect of benefiting the kidney, fixing the essence, and calming the fetus. S has been widely used clinically to nourish the liver and kidney, treat impotence, and prevent miscarriage since ancient times (Yang et al., 2016, Yang et al., 2017, Zhang et al., 2018). It was recorded in the “*De Pei Ben Cao*” that “nourish kidney qi, mixed with light salt water and stir-fried”, so *Semen Cuscutae* processed with salt solution has an enhanced effect in nourishing the kidney and calming the fetus. Previous studies showed that both S and Y were effective in improving embryo loss rate, uterine bleeding, and other related indexes in the KDM model rats, and the effect of Y was better than S (Wang et al., 2021) (Xu et al., 2023).

However, it remains unexplored for the active ingredients and potential molecule mechanism of S for the treatment of KDM. The characteristics of multi-component and multi-target make the modernization of Chinese medicine enter a bottleneck. The emergence of network pharmacology has changed the “a drug, a target, a disease” paradigm in drug research and development. The systemic and holistic construction of the “disease-phenotype-gene-drug” multilayer network from a network perspective to explore active compounds, relevant targets and disease-related pathways in traditional Chinese medicines, provides a feasible tool to elucidate the molecular mechanism of traditional Chinese medicine (TCM), in line with the holistic view, and treatment based on TCM syndrome differentiation (Wu and Wu 2015, Liu et al., 2021, Li et al., 2022, Pan et al., 2022, Sun et al., 2024).

In order to further explore the mechanism of Y in improving KDM, an integrative strategy featuring serum pharmacology coupled with network pharmacology were used in this study. Serum pharmacology was employed to identify the components that are absorbed into the blood which were commonly considered as the potential bioactive compounds. Furthermore, these components were used to construct an active ingredient-target-pathway network for KDM using network pharmacology approach, yielding the prediction that Y may regulate the various signaling pathway to ameliorate KDM. The animal pharmacodynamics were used to further evaluate the effect of Y on improving abortion in KDM. The specific process was shown in graphical

abstract. The active ingredients and mechanism of Y in improving KDM were studied, which provided a scientific basis for further elucidating the theory of TCM that the “salt system enters the kidney, and the cellular vein is tied to the kidney”.

2. Materials and methods

2.1. Materials and chemicals

Hydroxyurea tablets (1C0153D05) were provided by Qilu Pharmaceutical Co., Ltd. (Jinan, China). Mifepristone tablets (05210302) were purchased from Jiulong Humanwell Pharmaceutical Co., Ltd. (Wuhan, China). Progesterone Capsules (019283473) were supplied by Zhejiang Xianju Pharmaceutical Co., Ltd. (Zhejiang, China). The muriatic acid (20190905), formic acid (20190321), and ethyl alcohol (20190905) were purchased from Sinopharm Chemical Reagent, Co., Ltd. (Beijing, China). All other chemicals were of analytical grade and used according to standards. Enzyme-linked immunoassay (ELISA) kits for estradiol (E2, Lot No. JL20220001), and progesterone (P, Lot No. JL202200703) were provided by Shanghai Jianglai Biotechnology Co., Ltd. (Shanghai, China).

Semen Cuscutae: *Semen Cuscutae* herbal decoction pieces were purchased from Bozhou Xiehecheng Slices Factory Co., Ltd (Bozhou, China) and confirmed as the dry matured seed of *Cuscuta australis* R. Br. or *Cuscuta chinensis* Lam. of Convolvulaceae family by Professor Liu Shoujin (Anhui University of Traditional Chinese Medicine). Previous studies have evaluated the quality of the characteristic profiles of S and Y (Supplementary Figs. 3-4 and Supplementary Table 2).

2.2. Animals

Female and male specific pathogen free (SPF) grade Sprague-Dawley (SD) rats (200 ~ 220 g) were provided by Anhui Experimental Animal Center [No. Scxk (Wan) 2013-002]. All experiments were approved by the Committee on the Ethics of Animal Experiments of Anhui University of Chinese Medicine. Clean grade standard feeding, constant humidity and temperature, water and standard feed for animals to eat freely, continuous observation for a week without abnormalities in the group experiment.

2.3. Preparation of water extract of *Semen Cuscutae* processed with salt solution

Semen Cuscutae processed with salt solution: Take clean S, mix with salt solution, (2 g of salt per 100 g of S). After the salt solution was absorbed thoroughly, heat on a mild fire, fry it until it bulges slightly, take it out, and let it cool.

Water extract of *Semen Cuscutae* processed with salt solution: Soak the Salt-processed *Semen Cuscutae* in water for 30 min. Next, it was decocted twice with boiling water (1:10 and 1:8), 30 min for each, and then filtered. The filtrate was combined and concentrated to 0.075 g/mL.

2.4. Serum pharmacology analysis

2.4.1. Preparation of rat serum samples

The 9 female Sprague-Dawley rats were randomly divided into a blank group (B group), Raw products of *Semen Cuscuta* (S) group, and *Semen Cuscutae* processed with salt solution (Y) group, with three rats in each group. In this experiment, the medium dose of 10.8 g/kg was chosen for administration. The medium dose was 10 times the equivalent dose. The rats were orally administered twice daily for 3 days. Group B was fed normally. The blood was collected from the orbital plexus of rats at 30 and 60 min after the last administration, respectively. Then centrifuged at 3500 r/min for 10 min at 4°C after resting for 30 min, and the supernatant was extracted to obtain serum samples.

400 μL of each serum sample was taken; 40 μL hydrochloric acid (2 mol/L) was added, vortex shaken for 1 min, the samples were incubated at 4°C for 15 min, repeat vortex resting four times and dry by nitrogen blowing; The dried sample was dissolved in 200 μL of 80 % methanol and centrifuged at 4 °C for 10 min (12000 rpm). Finally, the collected supernatant was used to perform UHPLC-Q/TOF-MS analysis.

2.4.2. Chromatographic conditions

Sample analysis was performed on the UHPLC (Nexera UHPLC LC-30A) system was coupled. The column was Waters UPLC BEH C18 (2.1 mm \times 100 mm, 1.7 μm). Flow rate of 0.4 mL/min, injection volume of 3 μL . The mobile phase consisted of 0.1 % formic acid water (A) and 0.1 % formic acid acetonitrile (B) with a gradient as follows: 0–3.5 min, 95–85 % A; 3.5–6 min, 85–70 % A; 6–6.5 min, 70 % A; 6.5–12 min, 70–30 % A; 12–12.5 min, 30 % A; 12.5–18 min, 30–0 % A; 18–22 min, 0 % A.

2.4.3. Mass spectrometer conditions

The AB 5600 Triple TOF mass spectrometer is capable of primary and secondary mass spectrometry data acquisition based on the IDA function under the control of the control software (Analyst TF 1.7, AB Sciex). In each data acquisition cycle, the most intense molecular ions with an intensity greater than 100 were selected to obtain the MS/MS data. The bombardment energy: 40 eV, collision energy difference: 20 V, 15 secondary spectra every 50 ms. The ESI ion source parameters were set as follows: nebulization air pressure (GS1): 55 psi, auxiliary air pressure: 55 psi, air curtain air pressure: 35 psi, temperature: 550 °C, spray voltage: 5500 V (positive ion mode) or –4000 V (negative ion mode).

2.4.4. UHPLC-Q/TOF-MS data analysis

The XIC Manager tool in PeakView software was used for post data acquisition analysis. A database of prototypical components of *Semen Cuscutae* in blood was established basis on the in vitro screened chemical compositions, containing name, molecular formula, exact molecular weight, retention time, etc. Blank serum as well as drug-containing serum samples of S/Y were imported into the XIC Manager tool in PeakView software with the methodological parameters for data processing as XIC intensity > 50 counts, plus or minus error at ± 5 ppm, and retention time within the specified time. The mol formula of the screened compounds was then imported, and the secondary fragment ions were matched to the structure of the components in the light of the literature as well as the cleavage pattern, and a match of > 80 % was considered reasonable.

2.5. Network pharmacology

2.5.1. Target prediction of Y and KDM target screening

The structural formulas of the 13 Y components absorbed into blood were downloaded from PubChem (<https://pubchem.ncbi.nlm.nih.gov/>), and the component potential targets were obtained from the TCMSP (<https://old.tcmsp-e.com/tcmsp.php>) and Swiss Target Prediction (<https://www.swisstargetprediction.ch/>). The targets with probability > 0.5 were selected. GeneCards Human gene database (GeneCards) (<https://www.genecards.org/>) and Online Mendelian Inheritance in Man (OMIM) (<https://www.genecards.org/>) were used to search the related genes of KDM by searching for keywords, “recurrent spontaneous abortion, abortion and miscarriages”. Finally, the above targets are standardized as GeneSymbol through UniProt database (<https://www.uniprot.org/>). In order to assess the interaction between the targets of SS and KDM, common targets were obtained using Venny 2.1 (<https://bioinfogp.cnb.csic.es/tools/venny/>), and then the component-target-disease pathway network were performed using the Cytoscape 3.7.2 software.

2.5.2. Protein-protein interaction (PPI) construction and analysis

The common targets between the components and the disease were

imported into the STRING (<https://string-db.org/>). The parameters were set to “Homo sapiens” to obtain PPI network relationship maps and related network parameters. Import the obtained network parameters into Cytoscape 3.7.2 software to construct and visualize the PPI network.

2.5.3. GO and KEGG analysis

Metascape database (<https://metascape.org/>) was used for performing Gene Ontology (GO) enrichment analysis including biological processes (BP), molecular function (MF), and cellular component (CC) and Kyoto Encyclopedia of Genes and Genomes (KEGG) enrichment analysis. Correlation results were obtained with $P < 0.01$ as the screening condition.

2.5.4. “Ingredients–target–pathway” network construction

In order to analyze the action mechanism of SS active ingredients to improve KDM, the Cytoscape 3.7.2 software was used to construct “ingredients–target–pathway” network and determine the core targets in the pathway and the main entry components for treating KDM based on network parameters component.

2.5.5. Molecular docking

Chemical structures of compounds were available in PubChem (<http://pubchem.ncbi.nlm.nih.gov/>) and crystal structures of proteins were extracted from the RCSB Protein Data Bank (<https://www.rcsb.org/>). Through Pymol software, the solvent molecules in the target are removed, and the steps of hydrogenation, electron addition, and ROOT are performed on the target and through Autodock software. The processed protein and chemical structures were imported into AutoDockTools for docking experiments.

2.6. Pharmacodynamic experiment

2.6.1. Animal model construction and grouping and morphological observation

The female and male rats were mated (mating ratio 2:1). Vaginal smears of female rats were examined daily in the early morning hours. Day 0 of pregnancy is defined by the presence of a large number of sperm on the vaginal smear or the dropping of a vaginal plug. Finally, 40 pregnant rats were screened and randomly divided into the following five groups ($n = 8$): Control group (C), Model group (M), Positive drug group (P), Raw products of *Semen Cuscuta* (S) group, *Semen Cuscutae* processed with salt solution (Y) group. Hydroxyurea combined with mifepristone by gavage was used to establish a KDM model (Wang et al., 2021). The model and each treatment group were given hydroxyurea (450 mg/kg) daily in the morning, and the corresponding therapeutic drug was administered in the afternoon for each treatment group (positive drug: 18 mg/kg progesterone capsules; 10.8 g/kg water extract of S; 10.8 g/kg water extract of Y) for 10 days. Except for the control group, mifepristone was given on day 11 at a dose of 3.75 mg/kg. After 24 h of mifepristone administration, serum and tissue samples were obtained from each group of rats after anesthetized by intraperitoneal injection with pentobarbital (30 mg/kg).

After anesthetizing the rats, the uterus was taken and weighed after stripping the surrounding fat and other tissues to observe the morphology of the embryo and uterus. The criteria for determining miscarriage as follows: uterine morphology, color, intrauterine changes; number of normal embryos and number of aborted embryos. Normal embryos: the uterus was thick as a string of beads, pink or light red in color. The size of the fetal mouse was seen to be consistent with gestational age after dissection. The embryo was intact and the heartbeat of the fetal mouse could be observed, and no stasis of blood was seen. Partial abortion: stasis of blood was seen in the uterine cavity and the embryo was incomplete. Complete abortion: significant weight loss in the mother, bamboo-like changes in the uterus, obvious fatigue or necrotic embryos seen in the uterine cavity, or only the embryo bed site

was seen, no embryo was seen, or the embryo was dark brown, or there was vaginal bleeding.

2.6.2. Collection and preparation of samples

Pentobarbital (30 mg/kg body weight) was injected intraperitoneally to anesthetize the rats. Blood was collected from the abdominal aorta. Then, it was centrifuged at 3,500 rpm and 4 °C lasting for 15 min. Supernatant was aspirated, then stored at -80 °C.

The decidual tissue was separated from the uterine embedding site, and the entire meconium tissue was separated from the embryo and its embedding site, washed, absorbed water, and fixed with 4 % paraformaldehyde liquid fixative.

2.6.3. Measurement of embryo loss rate and uterine bleeding

Embryo loss rate (ELR): the uterus of intact pregnant rats was removed and opened longitudinally from the uterine horns. And the total number of fetuses, live fetuses and abortions in each group of pregnant rats in the uterus were recorded. The embryo loss rate was calculated. $ELR = \text{number of aborted embryos} / (\text{number of aborted embryos} + \text{number of normal embryos}) \times 100 \%$.

Uterine bleeding (UB): take 20 μ L of rat venous blood, add 4 mL of 5 % NaOH and mix well. Collect the cotton ball containing the uterine blood of a rat in an EP tube, add an appropriate amount of 5 % NaOH (4 ~ 7 mL) according to the actual situation of bleeding, the blood stain of cotton ball were soaked and scrubbed until the eluate was colorless. The absorbance (A) of the extracts and the rat venous blood were measured at 546 nm using 5 % NaOH solution as blank control. Vaginal bleeding (μ L) = volume of venous blood \times (A_{uterine dipstick} \times V2) / (A_{venous blood} \times V1), V1: dilution of venous blood; V2: amount of NaOH used for extracting uterine blood.

2.6.4. Histopathology

To evaluate histological changes in the decidual tissue, fixed in 4 % paraformaldehyde, followed by paraffin embedded sections, before being cut into 4 μ m sections, and stained with hematoxylin and eosin (H&E). Pathological changes in the decidual tissues were observed by light microscope.

2.6.5. Immunohistochemical detection of decidual tissue

The decidual tissue sections were then incubated with primary antibodies at the following concentrations: VEGF antibody (1:100), PI3K antibody (1:100), AKT antibody (1:100), p-PI3K antibody (1:100), p-AKT antibody (1:100) followed by the necessary secondary antibodies according to the appropriate IHC staining protocol. These sections were then observed by light microscopy. For the negative controls, the primary antibody was replaced with 0.01 M phosphate buffered solution (PBS). The intensity of staining was determined by analyzing the integrated optical density (IOD) using an image analysis system (JD-801). large IOD values tend to be brownish-yellow, indicating dark staining and strong protein expression, while small IOD values are darker, indicating light staining and weak protein expression. $IOD = \text{area density} \times \text{average optical density}$.

2.6.6. Detection of biochemical indices in rat serum

Enzyme-linked immunosorbent assay (ELISA) was used to test the content of progesterone (P), estradiol (E2) and vascular endothelial growth factor A (VEGF-A) in serum according to the manufacturer's instructions. Optical density (OD) values were measured at 450 nm using a microplate reader.

2.7. Statistical analysis

All data are expressed as means \pm standard deviation (SD). One-way analysis of variance (ANOVA) was used to compare statistical significance. Statistical significance was set at $P < 0.05$. Analysis and graphing were carried out through GraphPad Prism (version 8.0, GraphPad

Software, USA) and SPSS (version 23.0, IBM, USA).

3. Results

3.1. Analysis of serum components in rats

Using the results of the previous analysis of the in vitro components of *Semen Cuscuta* as a reference (Huang et al., 2022), the in vivo components were identified. As shown in Fig. 1, typical total ion chromatograms (TICs) of drug-containing serum were analyzed in positive and negative ion mode. A total of 13 chemical compounds absorbed into blood were detected by comparison, which includes flavonoids, volatile oils, phenolic acids, and other classes of compounds are summarized in Table 1. However, the metabolites in serum were not identified and classified given the complexity of the metabolites of herbal compounds. Meanwhile, multivariate statistical analysis was performed on the serum constituents of *Semen Cuscuta* before and after salt processing, the data was introduced into SIMCAP 14.1 for principal component analysis (PCA) score plot and orthogonal partial least squares discriminate analysis (OPLS-DA) as shown in Fig. 2, the serum constituents of S and Y were automatically clustered into 2 categories, indicating good variability between them. The intercept values of R²X, R²Y and Q² were 0.513, 0.99 and -0.892 all less than 1, the fitting validation results proved that there was no over-fitting and the established mathematical model is stable.

VIP analysis and *t*-test were performed on the components in serum of *Semen Cuscutae* before and after salt-processed, and the difference components in serum of raw *Semen Cuscutae* and *Semen Cuscutae* processed with salt solution were screened based on the principle of VIP > 1 and $P < 0.05$. The results, as shown in Table 2, showed that a total of seven compounds showed a significant difference, of which four compounds, including kaempferol, apigenin, kaempferol-3-O- β -D-glucuronide, and Luteolin, showed a significant increasing trend, and 3 of the compounds including linoleic acid, linolenic acid, and oleic acid showed a significant decreasing trend.

3.2. Network pharmacology analysis

3.2.1. Construction of the component-target-disease network and protein-protein interaction (PPI) network

Based on the 13 components of *Semen Cuscutae* processed with salt solution absorbed into blood identified in Table 1, the serum components were used to predict the targets of Y for improving KDM using a network pharmacology approach. Finally, 177 targets related to the components of Y were identified using the Swiss Target Prediction website. Using Gene Cards and the OMIM database, 2303 disease targets associated with miscarriage were obtained. Combining the targets related to active compounds of Y with the targets of KDM, and 92 potential targets for Y against KDM was obtained. (Fig. 3A). Next, 92 overlapping targets were imported into Cytoscape 3.7.2 software to construct the component-target-disease network, as shown in Fig. 3B, with 88 nodes and 145 edges, in which the orange diamond represents the Y, the yellow circle represents the blood component, and the green square represents the gene.

The 92 overlapping components and disease targets were imported into the STRING database to construct the PPI network. The PPI network has 91 core targets and 1099 edges (Fig. 3C), where the topological parameter degree of network analysis is the center of the node, which reflects the connectivity of the targets involved in the pathological process of the disease, meaning that the larger the value the more involved in the disease process (Cheng et al., 2022). With a degree value ≥ 39 as the screening condition, ultimately, a total of 18 key targets were obtained, including TPP53, AKT1, TNF, IL6, VEGFA, CASP3, JUN, EGFR, etc., as shown in Table 3.

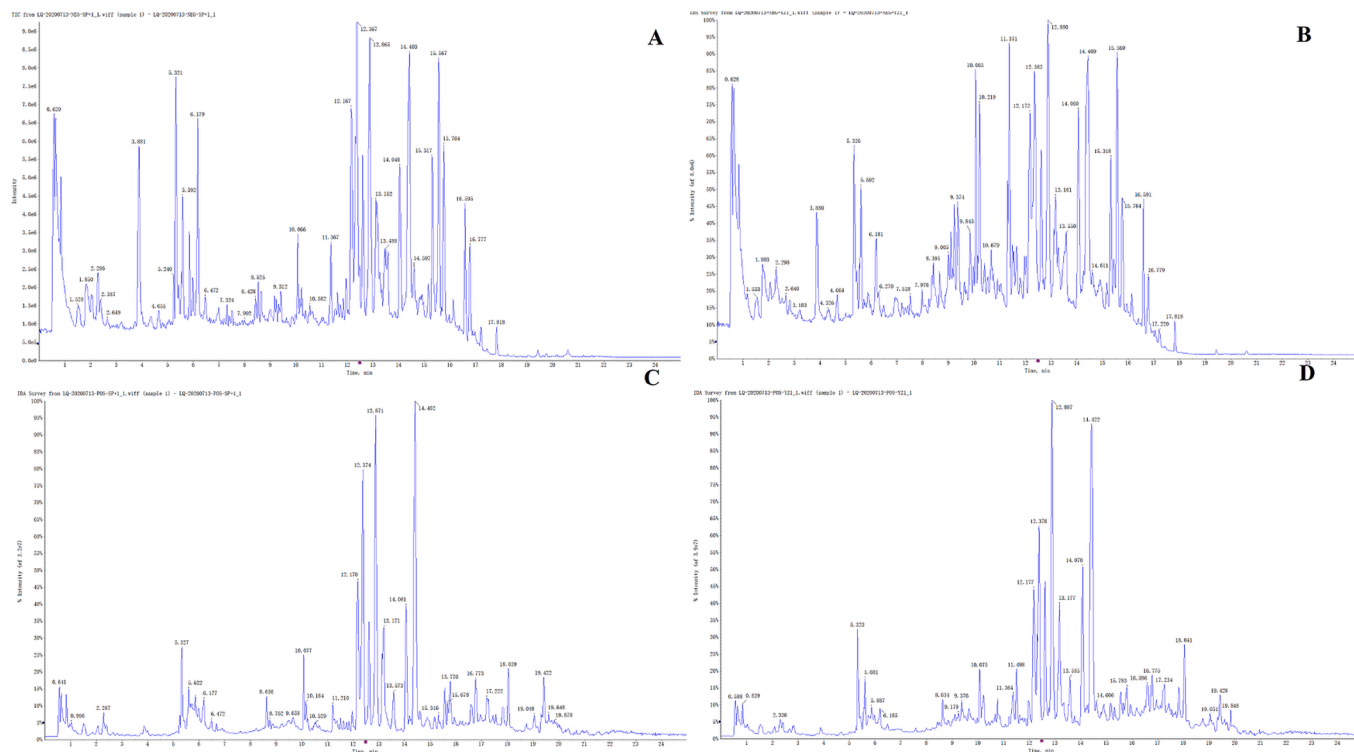


Fig. 1. Total ion chromatogram of blood components before and after salt-processed of *Semen Cuscutae*. Total ion flow diagram of the blood component of (A) S and (B) Y in negative ion mode. Total ion flow diagram of the blood component of (C) S and (D) Y in positive ion mode.

Table 1
Identification of the components in serum of *Semen Cuscutae* before and after salt-processing by UPLC-Q/TOF-MS.

NO.	Name	Fomula	RT (min)	Mass (Da)	Negative ion				Positive ion				Fragment mass	
					M-H	Error (ppm)	S	Y	M+H	Error (ppm)	S	Y	Negative	Positive
1	Kaempferol	C ₁₅ H ₁₀ O ₆	8.11	286.04774	285.03773	0.5	+	+	N.A.	N.A.	+	+	285.0406	287.0537
													185.0602	153.0176
2	Kaempferol-3-glucuronide	C ₂₁ H ₁₈ O ₁₂	6.05	462.07983	461.07181	-1.6	+	+	463.08712	0	+	+	461.1832	463.0925
													285.0401	287.0544
3	Luteolin	C ₁₅ H ₁₀ O ₆	7.96	286.04774	285.03773	-0.1	+	+	N.A.	N.A.	-	-	285.0323	-
4	Dicaffeoylquinic acid	C ₂₅ H ₂₄ O ₁₂	10.16	516.12678	515.12128	3.5	+	+	N.A.	N.A.	-	-	515.1203	-
													447.1332	
5	Stearic acid	C ₁₈ H ₃₆ O ₂	17.89	284.27153	283.26423	-0.1	+	+	285.27874	-0.2	+	+	283.2658	285.3642
6	Apigenin	C ₁₅ H ₁₀ O ₅	7.94	270.05282	269.04555	-1	+	+	271.0609	2.9	-	-	269.0329	271.0604
													225.0547	253.0538
													117.0342	153.0313
													151.0040	
7	Palmitic acid	C ₁₆ H ₃₂ O ₂	16.59	256.24023	255.2328	-0.6	+	+	257.24769	0.7	+	+	255.2337	257.1320
8	Linolenic acid	C ₁₈ H ₃₀ O ₂	15.76	278.22458	277.21748	0.6	+	+	279.2317	0.4	+	+	279.0960	281.9456
9	Linoleic acid	C ₁₈ H ₃₂ O ₂	14.84	280.24023	279.23322	0.9	+	+	281.24746	-1	+	+	281.2472	283.3895
													263.2367	
													245.2270	
10	Oleic acid	C ₁₈ H ₃₄ O ₂	16.74	282.25588	281.24888	1	+	+	283.26305	-2.6	+	+	281.2497	283.1077
11	(S) -11-Hydroxyhexadecanoic acid	C ₁₆ H ₃₂ O ₃	14.96	272.23515	271.22792	0.2	+	+	N.A.	N.A.	-	-	271.2269	-
													253.2174	
													225.2209	
12	α-Caryophyllene	C ₁₈ H ₃₀	15.5	246.23475	N.A.	N.A.	-	-	247.24129	-0.5	+	+	-	247.0238
13	Methyl myristate	C ₁₅ H ₃₀ O ₂	15.88	242.22458	241.2173	-0.1	+	+	NA	NA	-	-	241.2156	
													157.9960	
													141.0240	

Note: S: Raw products of *Semen Cuscuta*; Y: Salt-processed *Semen Cuscutae*; NA: Undetected.

3.2.2. GO and KEGG analysis

The Metascape database was used to perform GO enrichment (biological processes, cellular components and molecular functions) and KEGG pathway analysis on 92 common targets to determine the biological properties and various mechanisms of SS on KDM target genes.

The results of GO enrichment analysis were obtained, in which 1181 were associated with BP, 45 were associated with CC, 117 were associated with MF as shown in Fig. 4A ~ C. The p-value represents the enrichment degree, the lower the p, the higher the -log10(p), the higher and more significant the enrichment and the bluer the color; the size of

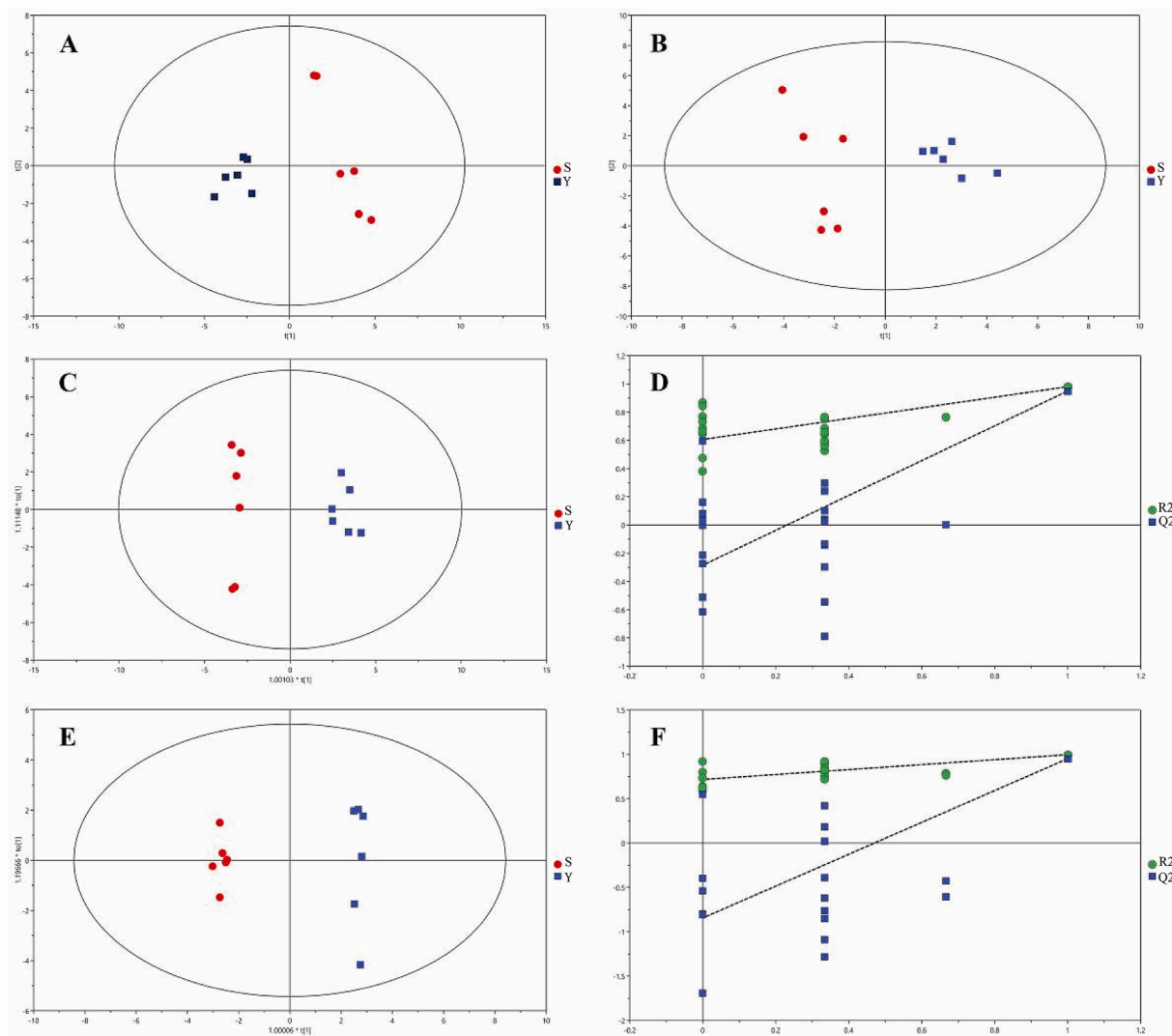


Fig. 2. Analysis of blood components of S and Y in positive and negative ion mode. PCA score plots (A) in positive ion mode and (B) in negative ion mode; OPLS-DA score plots (C) in positive ion mode and (E) in negative ion mode; permutation plots (D) in positive ion mode and (F) in negative ion mode.

Table 2

Information of differential blood entry prototypes of S-/Y- *Semen Cuscutae*.

NO.	RT (min)	Name	VIP	P	Trend (S vs Y)
1	8.11	Kaempferol	1.11	0.001	↑***
2	7.94	Apigenin	1.07	0.001	↑***
3	6.05	Kaempferol-3-glucuronide	1.10	0.001	↑***
4	7.91	Luteolin	1.11	0.001	↑***
5	14.84	Linolenic acid	1.10	0.001	↓***
6	15.76	Linoleic acid	1.04	0.001	↓***
7	16.78	Oleic acid	1.11	0.001	↓***

Note: “↑” response strength increases after processing; “↓” strength decreases after processing; “***” $P < 0.05$; “****” $P < 0.001$.

the circle indicates the number of genes enriched under the function. The results showed that the components of Y absorbed into blood were involved in cell growth and development, proliferation and apoptosis, and protein binding in the treatment of miscarriage. Here we found that BP enrichment was mainly involved in hormonal response, oxidative stress response, steroid hormone response; CC enrichment was mainly involved in serine/threonine protein kinase complex, cell cyclin-dependent protein kinase holoenzyme complex. Homodimerization activity of proteins, oxidoreductase activity, kinase binding was closely related to MF enrichment.

KEGG pathway analysis yielded 168 enrichment terms ($p < 0.01$), and the top-ranked KEGG pathways were selected based on p -value, as shown in Fig. 4D and Table 4. The significantly enriched KEGG pathways were PI3K-Akt signaling pathway, p53 signaling pathway, apoptosis, TNF signaling pathway, and HIF-1 signaling pathway. The more target genes on the pathway, the more Y may exert therapeutic effects by regulating these signaling pathways.

3.2.3. “Ingredients–target–pathway” network construction

All the targets on the pathway obtained from KEGG enrichment analysis were imported into Cytoscape 3.7.2 to map the component–target–pathway network and analyze the parameters such as degree, betweenness and closeness of components and targets. As shown in Fig. 3D, the network contains 93 nodes (10 ingredients, 29 signaling pathway, and 54 targets) and 340 edges. Each blood component corresponds to multiple targets, and each target corresponds to multiple components, reflecting the multi-component, multi-target improvement of KDM by Y.

Among them, luteolin (degree 33, medium 0.2212898, tightness 0.53488372). Therefore, luteolin was predicted to be the main active component of this blood component for the treatment of KDM, followed by kaempferol, and palmitic acid. This suggests that the pathways act in concert with each other through shared targets. Therefore, it is

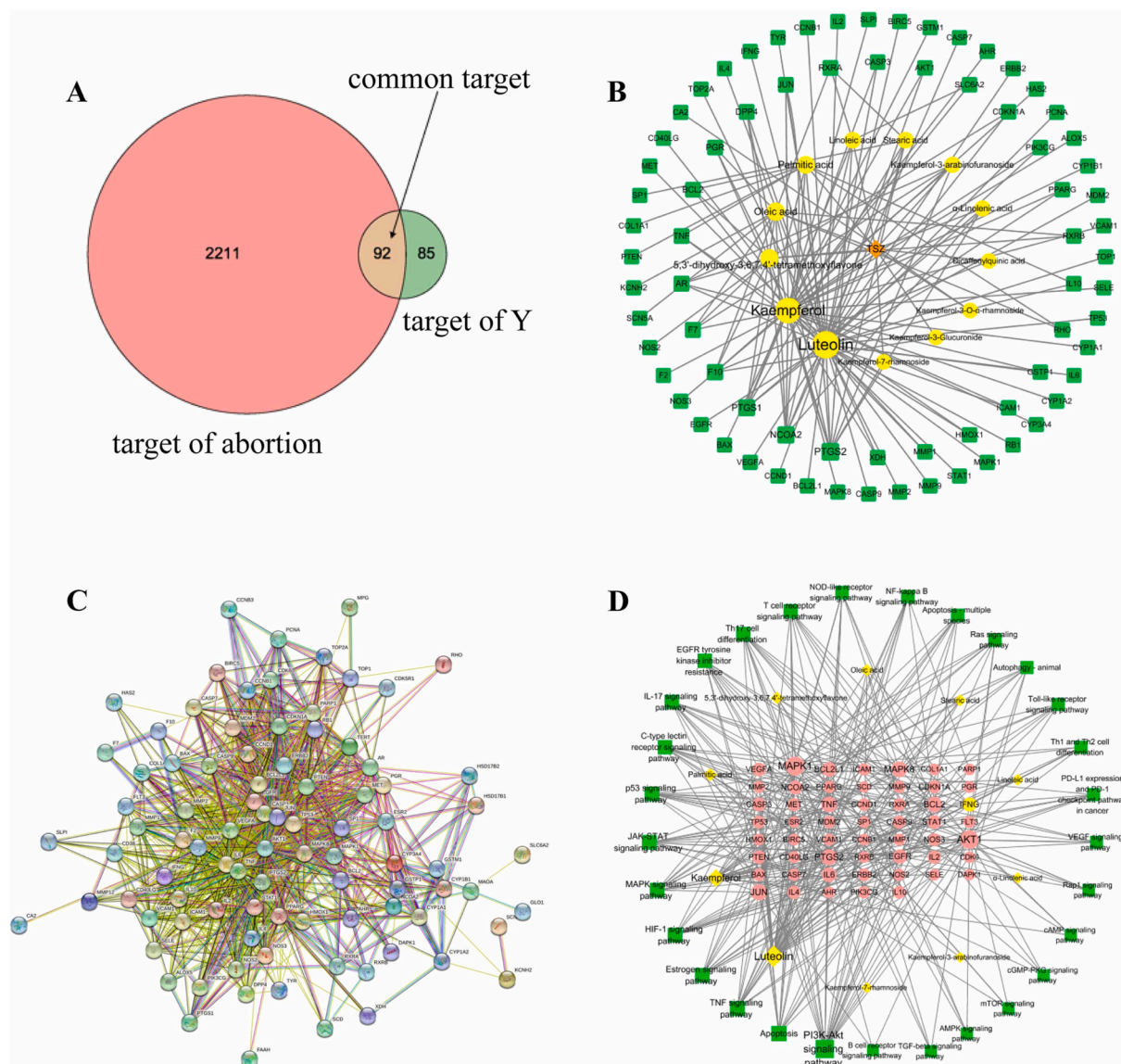


Fig. 3. (A) Venn diagram of Y and kidney deficiency miscarriage targets; (B) Y-active components-disease targets; (C) protein–protein interaction (PPI) network; (D) Ingredients–target–pathway network.

Table 3

Topological parameters of 18 targets at the top degree in PPI network.

Number	Gene Symbol	Betweenness Centrality	Closeness Centrality	Degree
1	TP53	0.0685116	0.76271186	65
2	AKT1	0.07014841	0.75630252	64
3	TNF	0.06219785	0.72580645	61
4	IL6	0.05579886	0.72580645	59
5	CASP3	0.02831991	0.6870229	54
6	VEGFA	0.02453724	0.69767442	54
7	JUN	0.02875544	0.67669173	52
8	EGFR	0.02552611	0.68181818	51
9	PTGS2	0.03309025	0.66176471	50
10	MMP9	0.02408114	0.65693431	49
11	PPARG	0.03670975	0.65693431	47
12	CCND1	0.01896063	0.63380282	46
13	PTEN	0.01258186	0.64748201	46
14	BCL2L1	0.01051118	0.63829787	44
15	ERBB2	0.011503	0.63829787	44
16	MAPK8	0.00774929	0.625	42
17	IL10	0.00893231	0.6122449	40
18	MMP2	0.01204864	0.60402685	39

suggested that all the pathways in Y act synergistically in the treatment of KDM.

3.2.4. Molecular docking

The top 5 core targets TP53 (PDBID: 3D06), AKT1 (PDBID: 1UNO), TNF (PDBID: 1EXT), IL6 (PDBID: 1ALU), VEGFA (PDBID: 1FLT) in the protein interaction network (PPI) degree ranking were selected as molecular docking genes based on the network pharmacology results and were molecularly docked with the compounds ranked in the top 5 degrees in the component-target network including: Luteolin, Kaempferol, Apigenin, Oleic Acid, Palmitic acid. The docking results of some representative are shown in Fig. 5A ~ E. The stability of binding between receptors and ligands depends on the binding energy, the lower the binding energy, the more stable the binding conformation of the receptor and ligand (Liu et al., 2023).

The highest docking score was obtained for VEGFA-Luteolin (vascular endothelial growth factor-Luteolin) with a binding energy of $-9.78 \text{ kcal}\cdot\text{mol}^{-1}$ (Fig. 5F), and the mean value of docking binding energy for all docking results was $-5.52 \text{ kcal}\cdot\text{mol}^{-1}$, which indicated a good binding activity between the blood component and the target site when molecular docking was performed. Five compound-molecule pairs

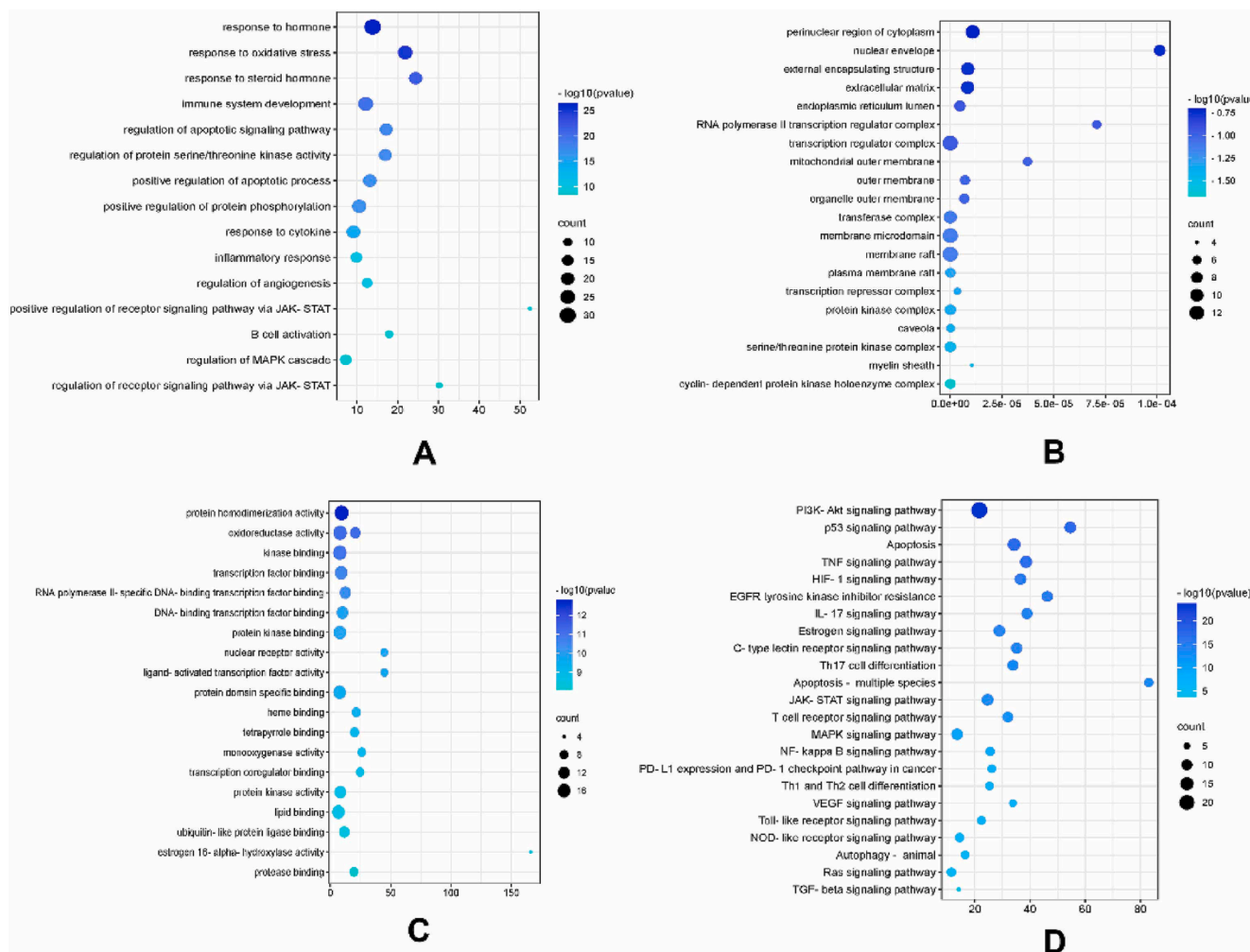


Fig. 4. Bubble chart of GO and KEGG enrichment analysis. (A) biological process, (B) cellular component, (C) molecular function, (D) KEGG enrichment result.

with docking binding energies below $-7.5 \text{ kcal}\cdot\text{mol}^{-1}$ were selected for docking patterns as well as pocket structure mapping. After molecular docking verification, it can be concluded that Luteolin was an important component of the serum component of Y, protein VEGFA is the core target of action of Y in the treatment of miscarriage, and other serum components of Y have certain or even strong binding ability to the targets acting on miscarriage.

3.3. Pharmacodynamic analysis

3.3.1. Establishment of KDM model and general observation

The 100 female rats and 50 male rats were mated (mating ratio 2:1), and the vaginas of the rats were coated with saline using a cotton swab early each morning, and the smear results are shown in Fig. 6A. A large number of keratinized epithelial cells during estrus. Due to individual differences and the inability to standardize the estrus period among rats, 40 fertile rats were finally selected for the hydroxyurea combined with mifepristone-induced kidney deficiency abortion model. Hydroxyurea combined with mifepristone induced KDM is a well-established and highly replicated model for testing the therapeutic potential of Y. The modeling results showed that the rats in the model group were huddled and less active, their body hair was thin, their food and water intake decreased, their body weight increased slowly or even decreased, their stools were loose and their anus was stuck with sticky and thin stools; or they had vaginal bleeding during the pregnancy, which was consistent with the performance of the rats with kidney deficiency, and these results indicated that the model of abortion induced by hydroxyurea in

rats with kidney deficiency was established successfully, while the rats in other groups were active as usual.

3.3.2. Morphological observation

According to Fig. 6B, the uterus of normal pregnant control (C) rats was thick as a string of beads and pink or light red, and the embryonic tissue was approximately the same in appearance; In the model group (M), the embryonic uterus of the rats showed bamboo-like changes, the uterine cavity showed obvious fatigue or necrotic embryos, or only the embryonic implantation site was seen without embryos, or the embryos were dark brown, or there was vaginal bleeding. In the positive drug group (P) the uterine of rats showed light red color, the embryos were basically uniform in size, with occasional individual unevenness, no bamboo-like changes, occasional bruising spots, and no obvious absorbed embryonic tissues were seen. The abortion of raw products of *Semen Cuscuta* (S) group, *Semen Cuscutae* processed with salt solution (Y) group were slightly improved. The uterus was light red or dark red, the size of embryonic tissues was basically the same, occasionally a small part of embryonic tissues was shrunken, no obvious bamboo-like changes were seen, and there was a small amount of bruising in the uterine cavity. Most of the embryonic tissues were not mechanized.

3.3.3. Calculation of embryo loss rate and uterine bleeding in rats with KDM

Statistical analysis of the number of embryos in each group showed that the rate of embryo loss in the M group was as high as 71.77 %, which was statistically significant compared to the C group ($P < 0.01$);

Table 4

The top 10 pathway enrichment of components in serum of *Semen Cuscutae* processed with salt solution.

ID	Description	Count	Gene ID
hsa04151	PI3K-Akt signaling pathway	23	AKT1 CCND1 BCL2 BCL2L1 CASP9 CDK6 CDKN1A COL1A1 EGFR ERBB2 FLT3 IL2 IL4 IL6 MDM2 MET NOS3 PIK3CG MAPK1 PTEN RXRA TP53 VEGFA
hsa04115	p53 signaling pathway	12	BAX CCND1 BCL2 BCL2L1 CASP3 CASP9 CCNB1 CDK6 CDKN1A MDM2 PTEN TP53
hsa04210	Apoptosis	14	PARP1 AKT1 BIRC5 BAX BCL2 BCL2L1 CASP3 CASP7 CASP9 JUN MAPK1 MAPK8 TNF TP53
hsa04668	TNF signaling pathway	13	AKT1 CASP3 CASP7 ICAM1 IL6 JUN MMP9 MAPK1 MAPK8 PTGS2 SELE TNF VCAM1
hsa04066	HIF-1 signaling pathway	12	AKT1 BCL2 CDKN1A EGFR ERBB2 HMOX1 IFNG IL6 NOS2 NOS3 MAPK1 VEGFA
hsa01521	EGFR tyrosine kinase inhibitor resistance	11	AKT1 BAX BCL2 BCL2L1 EGFR ERBB2 IL6 MET MAPK1 PTEN VEGFA
hsa04657	IL-17 signaling pathway	11	CASP3 IFNG IL4 IL6 JUN MMP1 MMP9 MAPK1 MAPK8 PTGS2 TNF
hsa04915	Estrogen signaling pathway	12	AKT1 BCL2 EGFR ESR2 JUN MMP2 MMP9 NOS3 PGR MAPK1 SP1 NCOA2
hsa04625	C-type lectin receptor signaling pathway	11	AKT1 IL2 IL6 IL10 JUN MDM2 MAPK1 MAPK8 PTGS2 STAT1 TNF
hsa04659	Th17 cell differentiation	11	AHR IFNG IL2 IL4 IL6 JUN MAPK1 MAPK8 RXRA RXRB STAT1

the rate of embryo loss was greatly reduced in each administration group compared to the M group, and the therapeutic effect was better in the Y group. The amount of uterine bleeding showed that the amount of uterine bleeding in the model group was significantly higher than that in the other groups. After administration of the corresponding drugs, the groups improved significantly, with the amount of uterine bleeding in the Y group being significantly lower than that in the S group. The specific values are shown in Table 5 and Fig. 7A and B.

3.3.4. Hormone e and VEGF-A levels in rat serum

As shown in Fig. 7C, D and E, compared with C group, the serum levels of estradiol, progesterone and VEGF-A were significantly lower ($P < 0.001$) in rats in group M; Compared with the M group, the estradiol,

progesterone and VEGF-A levels in the serum of rats in the P group were significantly higher ($P < 0.01$), and the serum of rats in the S and Y groups were significantly elevated compared with the M group ($P < 0.001$), with the Y being significantly higher than the S group.

3.3.5. Histopathology

As shown in Fig. 8, the cytoplasmic staining of the decidual tissue of the rats in the C group was uniform, with clear cell boundaries, tight columns and abundant blood vessels. In M group, the metaphase cells were degenerated and lost intercellular connections, some metaphase cells were necrotic, and the interstitial blood vessels were obviously reduced. The vascular morphology of the metaphase tissue of the rats in each administration group showed a trend of improvement, with closely arranged metaphase cells, intact glandular morphology, regular arrangement of interstitial cells, clear structure, uniform cytoplasmic staining and good vascular growth, which tended to the normal group. Among them, Y group showed the most obvious improvement.

3.3.6. Immunohistochemistry

As shown in Fig. 9, the positive expression of VEGF, PI3K, AKT, CD31, p-AKT, and p-PI3K was significantly decreased in M group compared with C group ($P < 0.01$). Compared with the model group, the protein expressions of all the administered groups were all back-regulated, and the expression of VEGF, PI3K, CD31, p-AKT, and p-PI3K in the Y group was higher than that in the S group, this result showed that Y had a significant improvement effect on kidney deficiency abortion rats.

4. Discussion

According to TCM, the main pathogenesis of this disease are kidney deficiency, essence deficiency, and lack of consolidation of the flushing process. Luo proposed the theory of “Kidney - Tiankui - Chong Ren - Uterus” as the female reproductive axis in Chinese medicine (Huang and Jiang 2021). This theory suggested that the kidney essence and kidney qi are full and depend on the Tiankui transformed by the innate kidney qi to arrive, the sea of blood overflows, the yin and yang meet, and the ligaments on the uterus gather the essence and blood of the internal organs in the two channels of Chong Ren and inject it into the uterus. This fully illustrates that the kidney is the master of reproduction and the essence of punching, the fullness of kidney qi is essential for normal fetal pregnancy. Sufficient Kidney qi could ensure the smooth flow of the uterus, abundant blood vessels in maternal-fetal interface contribute to

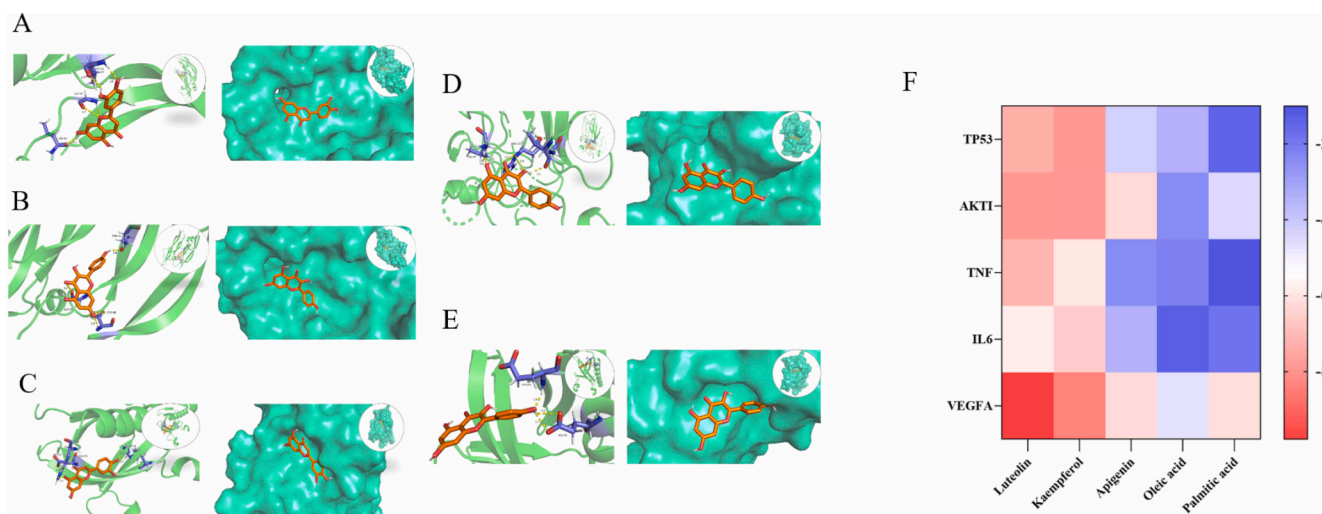


Fig. 5. (A) VEGFA-Luteolin, (B) VEGFA-Kaempferol, (C) AKTI-Luteolin, (D) TP53-Kaempferol, (E) AKTI-Kaempferol, (F) Heatmap shows docking scores of TP53, AKTI, TNF, IL-6, VEGFA combining to the five active ingredients of Y.

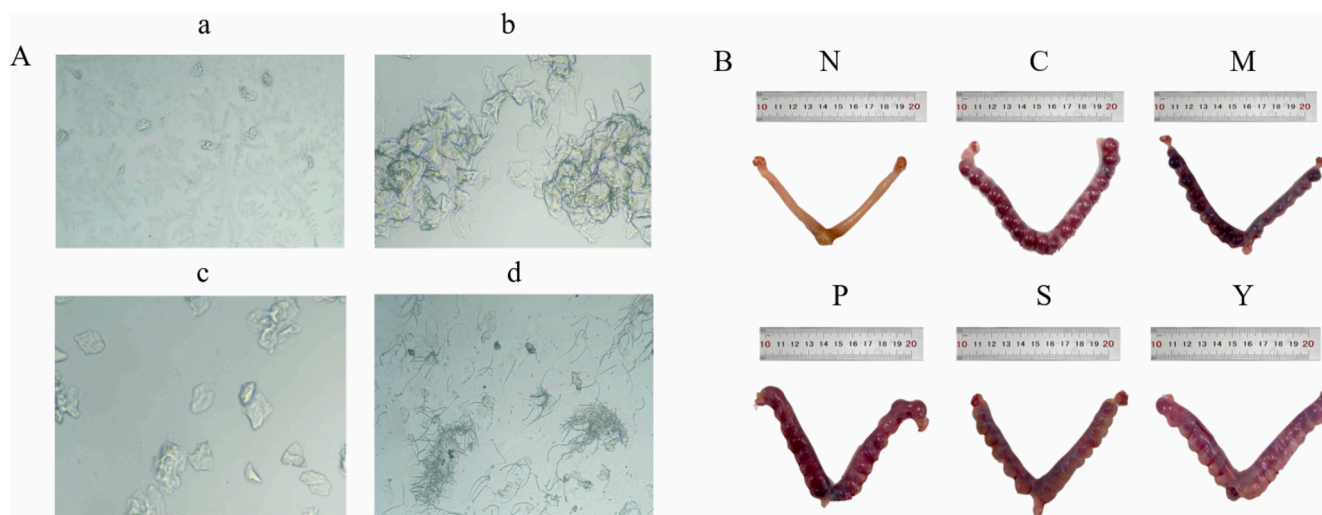


Fig. 6. (A) Micrograph of rat vaginal smear. (Light microscopy, 10 ×): (a) Interestrus, (b) oestrus, (c) late oestrus, (d) Vaginal sperm smear in rats; (B) Morphology of rat uterus: (N) Normal; (C) Control; (M) Model; (P) Progesterone group; (S) raw products of *Semen Cuscuta* group; (Y) *Semen Cuscutae* processed with salt solution group.

Table 5

Embryo loss rate and amount of uterine bleeding in pregnant rats. ($\bar{X} \pm S$).

Group	Number	Dosage (g. kg ⁻¹)	Embryo loss rate(%)	Amount of uterine bleeding
C	8	/	/	/
M	8	0.45	71.77 ± 21.67**	566.55 ± 3.62**
P	8	0.018	42.56 ± 23.37##	195.22 ± 9.56##
S	8	10.8	48.38 ± 18.56##	233.96 ± 4.53##
Y	8	10.8	40.37 ± 12.37##	205.03 ± 1.03##

Compare with the Control, * $P < 0.05$, ** $P < 0.01$; compared with the Model, # $P < 0.05$, ## $P < 0.01$.

the establishment of good maternal-fetal circulation (Mu et al., 2023). The cytokines are the ligaments on the uterus, which are crisscrossed and networked in the body. Kidney deficiency can trigger the obstructed uterine ligaments, stagnation of blood circulation, and eventually lead to an unstable fetus. The above discussion fully supports the theory that “the uterine ligament is tied to the kidney” (Huang et al., 2021, Zhou et al., 2022).

The theory of serum pharmacology points out that “it is the components that are absorbed into the blood that are the real bioactive substances that exert their effects”, these active components are delivered from blood to the target as mediators to produce pharmacological effects (Ma et al., 2017). In this study, we used UHPLC-Q/TOF-MS technique to analyze the serum of rats gavaged with aqueous decoction of Y in order to clarify its material basis. Furthermore, network pharmacology was used to predict the targets and mechanisms of the screened active components in serum. The results showed that a total of 13 prototype components were detected, kaempferol and luteolin are flavonoids compounds, which can reduce proliferation and inflammatory mediators in human pregnancy tissues by inhibiting NF-κB DNA binding activity and AP-1 pathway, ultimately improving miscarriage. (Wall et al., 2013).

Statistical analyses of the intensities of these 13 compounds revealed a total of seven significantly different constituents in serum of *Semen Cuscutae* before and after salt preparation, of which kaempferol, apigenin, kaempferol glucuronide, and lignocerotin showed a significant upward trend, whereas linolenic acid, linoleic acid, and oleic acid showed a significant downward trend. These compositional changes also directly lead to changes in the potency of *Semen Cuscutae* before and after concoction. For example, apigenin and kaempferol have the effects of inhibiting the proliferation of various cancer cells, anti-inflammatory

and anti-infective (Kashyap et al., 2022); dicaffeoylquinic acid (Gupta et al., 2022) protects the kidney and improves diabetes mellitus type 1, lignocerol has an oestrogen-like effect when used alone, and enhances the thickness of the endometrium as well as the height of its epithelial cells; Poplar flavonoids protect the testicular tissues and promote testosterone secretion, thereby improve the spermatogenic function of the testis (Imran et al., 2019). Based on these studies, it can be judged that the mechanism of the potentiation of *Semen Cuscutae* after salt preparation may be due to the synergistic effect of other classes of components, such as flavonoids and phenolic acids, which work in concert with each other to tonify the kidneys and calm the foetus.

The PPI network construction revealed that these 13 compounds may play a role in improving KDM by regulating TP53, AKT1, TNF, IL6, VEGFA, and other genes. VEGF, a growth factor with pro-angiogenic activity, is involved in the cascade reaction of ecdysteroid angiogenesis, is involved in regulating vascular permeability to promote endometrial edcysis, and plays an important role in the formation of the vascular network at the maternal-fetal interface (Guo et al., 2021, Jing et al., 2021). Modern medicine believes that a good immune microenvironment is necessary for a successful pregnancy and that any imbalance between proinflammatory and anti-inflammatory cytokines can lead to aberrant inflammation, which disrupts the stable immune microenvironment and threatened pregnancy (Kalagiri et al., 2016). Clinical studies have found that the levels of inflammatory factors in patients with miscarriage are significantly higher than in those with normal pregnancy, clinical studies have found that inflammatory factor (TNF-α and IL-6) levels are significantly higher in patients with miscarriage than in those with normal pregnancies, which also suggests that the elevated levels of inflammatory factors were associated with an increased risk of miscarriage (Kırıcı and Tanrıverdi 2021).

The results of target enrichment analysis by KEGG showed that the active targets were mainly concentrated in PI3K-Akt signaling pathway, p53 signaling pathway, TNF signaling pathway, which suggested that the targets were acting under the co-regulation of multiple pathways. Among them, PI3K-Akt signaling is one of the most prominent pathways, plays an important role in cell proliferation, apoptosis, and metabolism. Importantly, activation of the PI3K-Akt signaling pathway is importantly linked to the construction of the vascular network at the maternal-fetus interface which inhibits platelet agglutination, promotes Nitric Oxide (NO) secretion, stimulates vasodilation, and promotes blood circulation (Xie et al., 2019). Li showed that the activation of PI3K/AKT signaling pathway promoted the proliferation and migration of

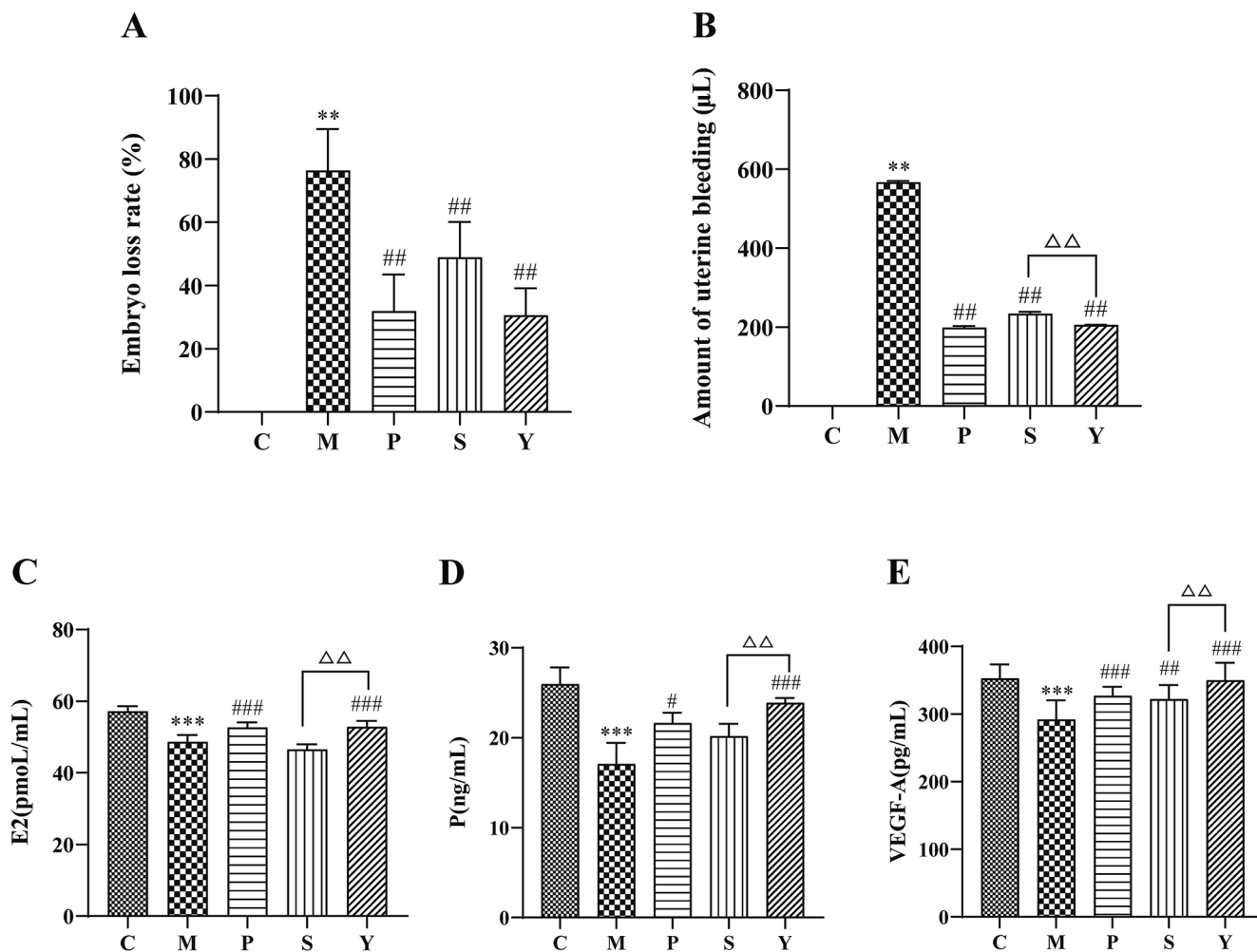


Fig. 7. Embryo loss rate (A) and amount of uterine bleeding (B) in pregnant rats. E2, P, VEGF-A content in the serum (C, D, E). Compared with the C group, * $P < 0.05$, ** $P < 0.01$, *** $P < 0.001$; Compared with the M group, # $P < 0.05$, ## $P < 0.01$, ### $P < 0.001$ Compare with the Y group, $\Delta P < 0.05$, $\Delta\Delta P < 0.01$, $\Delta\Delta\Delta P < 0.001$.

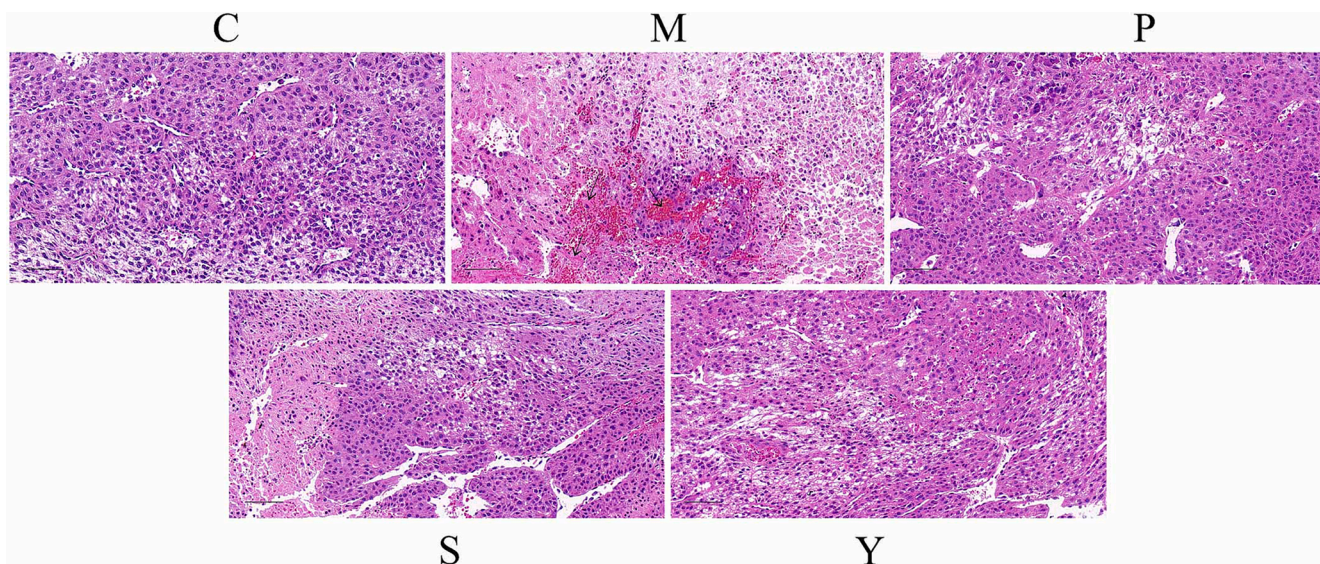


Fig. 8. Decidual tissue sections were stained with hematoxylin and eosin (H&E) for histopathologic analysis. Scale bars = 100 μm (Light microscopy, 20 ×): (C) Control group; (M) Model group; (P) Progesterone group; (S) raw products of *Semen Cuscuta* group; (Y) *Semen Cuscutae* processed with salt solution group.

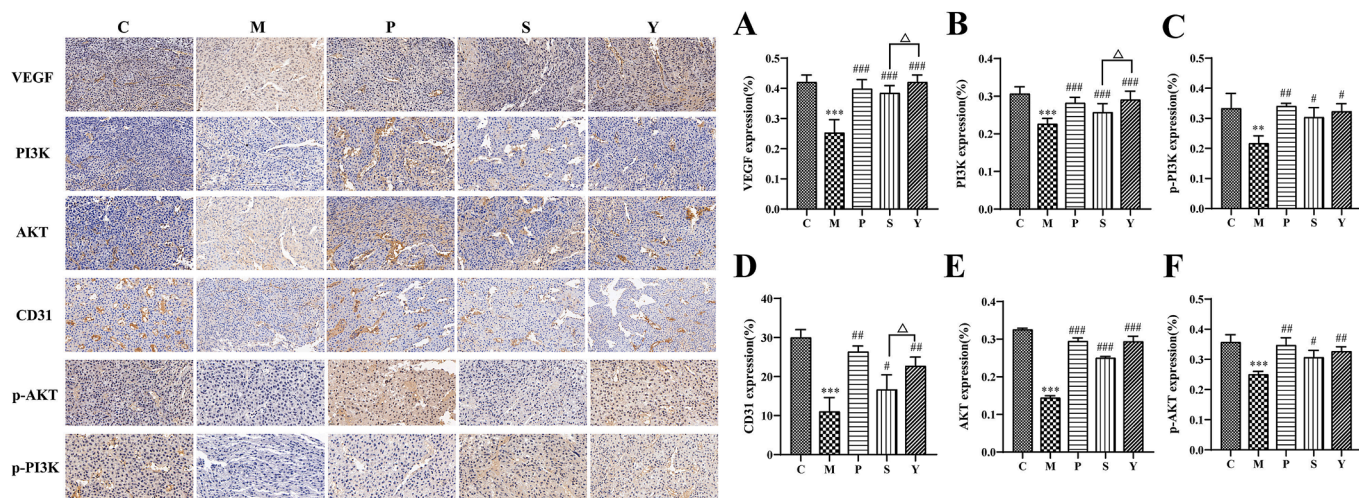


Fig. 9. The expression of (A)VEGF, (B)PI3K, (C)p-PI3K, (D)CD31, (E)AKT, and (F)p-AKT, and determined by immunohistochemical staining. Scale bars = 20 μm (Light microscopy, 40 ×). Compared with the C, *P < 0.05, **P < 0.01, ***P < 0.001; Compared with the M group, #P < 0.05, ##P < 0.01, ###P < 0.001; Compare with Y group ΔP < 0.05, ΔΔP < 0.01, ΔΔΔP < 0.001.

embryonic trophoblast cells, which had an important positive effect on the remodeling of uterine spiral arteries and the perfusion of placental blood (Li et al., 2019).

Based on the prediction of network pharmacology, further animal pharmacodynamic experiments were established using a rat model of KDM by instilling hydroxyurea in female rats and male rats after mating. The immunohistochemical results showed that the expression of proteins related to PI3K-AKT signaling pathway and VEGF were

significantly down-regulated in the model rats, however, these protein levels were up-regulated after treatment with S. As discussed above, VEGF is central in the cascade response of the vascular network at the maternal-fetal interface, and the PI3K/AKT signaling pathway is a key downstream mediator of VEGF. Specific binding of VEGF to its receptor leads to the activation of the PI3K/AKT signaling pathway, which further regulates angiogenesis (Li et al., 2016, Zhu et al., 2018). The decreased estrogens levels such as estradiol and progesterone in rats

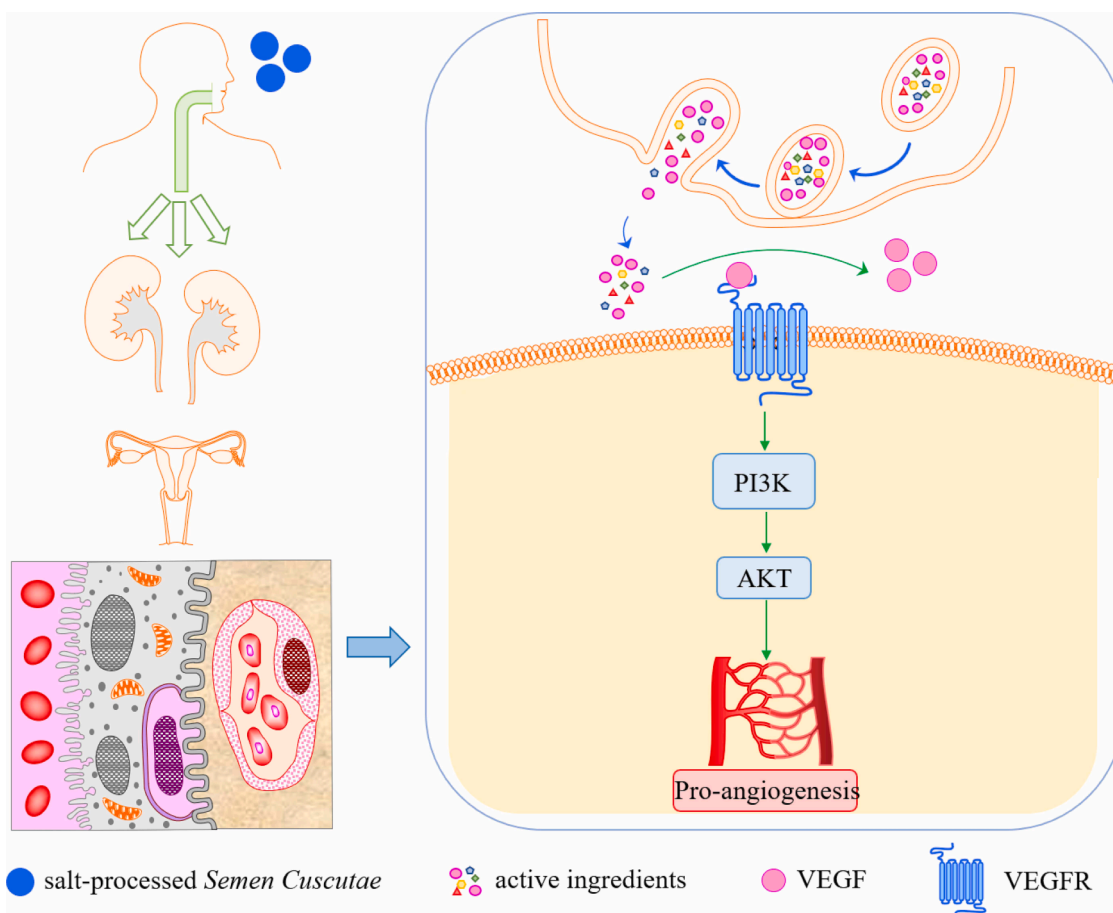


Fig. 10. Mechanism diagram for Y-improvement of KDM.

indicated the degeneration of their reproductive function and the possibility of miscarriage, while the progesterone levels were increased after the administration of S and Y, and the effect of Y was better than that of S. S has been widely used in the clinical treatment of the occurrence of miscarriage (Yang et al., 2020). The above results fully demonstrate that S can effectively improve the hormone levels and pathological changes in rats with KDM, and in addition the mechanism by which Y improves KDM may be related to the activation of VEGF-P13K/AKT signaling axis, which is basically consistent with the predicted results of network pharmacology (Fig. 10).

5. Conclusion

In conclusion, this study combined serum pharmacology and network pharmacology to determine the activity components of Y in improving KDM, these dozen active ingredients improved KDM by modulating targets, including TP53, AKT1, TNF, IL-6, VEGFA and interfering with PI3K/AKT signaling pathways which were found to play an important role in cell growth and development, apoptosis, and angiogenesis by enrichment analysis. The enrichment analysis was also verified by animal efficacy experiments. This study provides a basis for elucidating the mechanism of Y in improving KDM.

Author contributions

Xue Zhang, Yu Huang, Zhitong Yang performed the most of the experiments and wrote the manuscript; Baiyang Xu, Zilu Liu, Ximeng Ding, assisted in experiments and recorded the data; Qiumei Zhou, Gang Cao, Weidong Li, Chuanshan Jin, Shanshan Li, Xiaoli Wang reviewed the manuscript. Xiaoli Wang supervised the design of this study.

Declaration of competing interest

The authors declare that they have no known competing financial interests or personal relationships that could have appeared to influence the work reported in this paper.

Acknowledgements

This work was supported by National Natural Science Foundation of China (NSFC) (No. 82204623), Youth Science and Technology talents Cultivation Project of Anhui University of Chinese Medicine (No. 2021qny04), High-level Talents Program of Anhui University of Chinese Medicine (No. 20190108), Key Projects of Scientific Research in Anhui Universities (2022AH050471) and Heritage Base of TCM Processing Technology of NATCM of Anhui University of Chinese Medicine (No. RZ2200001251).

Appendix A. Supplementary material

Supplementary data to this article can be found online at <https://doi.org/10.1016/j.arabjc.2023.105456>.

References

Avant, R.F., 1983. Spontaneous abortion and ectopic pregnancy. *Prim. Care* 10, 161–172.

Cheng, Y., Xiao, M., Chen, J., et al., 2022. Quality assessment and Q-markers discovery of Tongshimai tablet by integrating serum pharmacology and network pharmacology for anti-atherosclerosis benefit. *Chin. Med.* 17, 103. <https://doi.org/10.1186/s13020-022-00658-9>.

Guo, X., Yi, H., Li, T.C., et al., 2021. Role of Vascular Endothelial Growth Factor (VEGF) in human embryo implantation: Clinical implications. *Biomolecules* 11. <https://doi.org/10.3390/biom11020253>.

Gupta, A., Atanasov, A.G., Li, Y., et al., 2022. Chlorogenic acid for cancer prevention and therapy: Current status on efficacy and mechanisms of action. *Pharmacol. Res.* 186, 106505 <https://doi.org/10.1016/j.phrs.2022.106505>.

HUANG, L. and S. CHEN, 2021. Curative effect of acupuncture for coordinating Chang-Ren and strengthening kidney combined with Yigong Yangpao Decoction on small follicular ovulation infertility and its effect on the function of the hypothalamus-

pituitary-ovarian axis. *Modern Journal of Integrated Traditional Chinese and Western Medicine.* 30, 160-163+203.

Huang, L., Gu, Y., Jiang, M., 2021. Analysis of the relationship between the theory of uterus, uterine vessels, uterine collaterals and endometrial receptivity. *Jilin J. Chinese Med.* 41, 854–857.

Huang, L., Jiang, M., 2021. Tonifying kidney and activating blood circulation for low endometrial receptivity from theory of Kidney-Tianguai-Chongren-Uterus reproductive axis. *Liaoning J. Trad. Chinese Med.* 48, 45–48.

Huang, Y., Yu, H., Xiong, J., et al., 2022. Chemical profiling of raw product of Semen Cuscuta and stir-baking Semen Cuscuta with salt solution based on UHPLC-Q /TOF-MS combined multivariate statistical analysis. *Chinese J. New Drugs* 31, 1542–1552.

Imran, M., Rauf, A., Abu-Izneid, T., et al., 2019. Luteolin, a flavonoid, as an anticancer agent: A review. *Biomed. Pharmacother.* = *Biomed. Pharmacother.* 112, 108612 <https://doi.org/10.1016/j.biopha.2019.108612>.

Jing, G., Yao, J., Dang, Y., et al., 2021. The role of β -HCG and VEGF-MEK/ERK signaling pathway in villi angiogenesis in patients with missed abortion. *Placenta* 103, 16–23. <https://doi.org/10.1016/j.placenta.2020.10.005>.

Kaczynski, P., Goryszewska, E., Baryla, M., et al., 2020. Prostaglandin F₂ α stimulates angiogenesis at the embryo-maternal interface during early pregnancy in the pig. *Theriogenology* 142, 169–176. <https://doi.org/10.1016/j.theriogenology.2019.09.046>.

Kalagiri, R.R., Carder, T., Choudhury, S., et al., 2016. Inflammation in complicated pregnancy and its outcome. *Am. J. Perinatol.* 33, 1337–1356. <https://doi.org/10.1055/s-0036-1582397>.

Kashyap, P., Shikha, D., Thakur, M., et al., 2022. Functionality of apigenin as a potent antioxidant with emphasis on bioavailability, metabolism, action mechanism and in vitro and in vivo studies: A review. *J. Food Biochem.* 46, e13950.

Kirci, P., Tanrıverdi, E.S., 2021. Effects of different progesterone doses on the concentrations of proinflammatory and anti-inflammatory cytokines in pregnant women with threatened abortion. *Cureus* 13, e19333.

Li, Z., Wang, B., Tang, L., et al., 2016. Quinazoline derivative compound (11d) as a novel angiogenesis inhibitor inhibiting VEGFR2 and blocking VEGFR2-mediated Akt/mTOR /p70s6k signaling pathway. *Iran. J. Basic Med. Sci.* 19, 411–416.

Li, X., Wei, S., Niu, S., et al., 2022. Network pharmacology prediction and molecular docking-based strategy to explore the potential mechanism of Huanglian Jiedu Decoction against sepsis. *Comput. Biol. Med.* 144, 105389 <https://doi.org/10.1016/j.compbiomed.2022.105389>.

Li, Z., Zhou, G., Jiang, L., et al., 2019. Effect of STOX1 on recurrent spontaneous abortion by regulating trophoblast cell proliferation and migration via the PI3K/AKT signaling pathway. *J. Cell. Biochem.* 120, 8291–8299. <https://doi.org/10.1002/jcb.28112>.

Liu, H., Li, X., Duan, Y., et al., 2021. Mechanism of gypenosides of *Gynostemma pentaphyllum* inducing apoptosis of renal cell carcinoma by PI3K/AKT/mTOR pathway. *J. Ethnopharmacol.* 271, 113907 <https://doi.org/10.1016/j.jep.2021.113907>.

Liu, Q.-H., Li, J.-Q., Tang, J.-W., et al., 2023. Identification of antidiabetic constituents in *Polygonatum odoratum* (Mill.) Druce by UPLC-Orbitrap-MS, network pharmacology and molecular docking. *Arab. J. Chem.* 16, 105032 <https://doi.org/10.1016/j.arabjc.2023.105032>.

Ma, F.X., Xue, P.F., Wang, Y.Y., et al., 2017. Research progress of serum pharmacology of traditional Chinese medicine. *Zhongguo Zhong yao za zhi = Zhongguo zhongyao zazhi = China J. Chinese Mater. Med.* 42, 1265–1270. <https://doi.org/10.19540/j.cnki.cjmm.20170224.010>.

Mu, Z., Shen, S., Tang, L., et al., 2023. Hyperin promotes proliferation, migration, and invasion of HTR-8/SVneo trophoblast cells via activation of JAK1/STAT3 pathway in recurrent spontaneous abortions. *Heliyon* 9, e12958. <https://doi.org/10.1016/j.heliyon.2023.e12958>.

Pan, H.T., Xi, Z.Q., Wei, X.Q., et al., 2022. A network pharmacology approach to predict potential targets and mechanisms of “Ramulus Cinnamomi (cassiae) - Paeonia lactiflora” herb pair in the treatment of chronic pain with comorbid anxiety and depression. *Ann. Med.* 54, 413–425. <https://doi.org/10.1080/07853890.2022.2031268>.

Sun, F., Liu, J., Xu, J., et al., 2024. Molecular mechanism of Yi-Qi-Yang-Yin-Ye against obesity in rats using network pharmacology, molecular docking, and molecular dynamics simulations. *Arab. J. Chem.* 17, 105390 <https://doi.org/10.1016/j.arabjc.2023.105390>.

Tan, S.Y., Hang, F., Purvarshi, G., et al., 2015. Decreased endometrial vascularity and receptivity in unexplained recurrent miscarriage patients during midluteal and early pregnancy phases. *Taiwan. J. Obstet. Gynecol.* 54, 522–526. <https://doi.org/10.1016/j.tjog.2014.10.008>.

Wahabi, H.A., Fayed, A.A., Esmaeil, S.A., et al., 2018. Progesterone for treating threatened miscarriage. *Cochrane Database Syst. Rev.* 8, Cd005943. <https://doi.org/10.1002/14651858.CD005943.pub5>.

Wall, C., Lim, R., Poljak, M., et al., 2013. Dietary flavonoids as therapeutics for preterm birth: luteolin and kaempferol suppress inflammation in human gestational tissues in vitro. *Oxid. Med. Cell. Longev.* 2013, 485201 <https://doi.org/10.1155/2013/485201>.

Wang, X., H. Gao, S. Tan, et al., 2021. An integrated approach to uncover quality markers of stir-baking Semen Cuscuta with salt solution preventing recurrent spontaneous abortion based on chemical and metabolomic profiling. *Journal of chromatography. B, Analytical technologies in the biomedical and life sciences.* 1177, 122727. <https://doi.org/10.1016/j.jchromb.2021.122727>.

Wu, X.M., Wu, C.F., 2015. Network pharmacology: a new approach to unveiling Traditional Chinese Medicine. *Chin. J. Nat. Med.* 13, 1–2. [https://doi.org/10.1016/s1875-5364\(15\)60001-2](https://doi.org/10.1016/s1875-5364(15)60001-2).

- Xie, Y., Shi, X., Sheng, K., et al., 2019. PI3K/Akt signaling transduction pathway, erythropoiesis and glycolysis in hypoxia (Review). *Mol. Med. Rep.* 19, 783–791. <https://doi.org/10.3892/mmr.2018.9713>.
- Xu, B., Z. Yang, X. Zhang, et al., 2023. 16S rDNA sequencing combined with metabolomics profiling with multi-index scoring method reveals the mechanism of salt-processed Semen Cuscuta in Bushen Antai mixture on kidney yang deficiency syndrome. *Journal of chromatography. B, Analytical technologies in the biomedical and life sciences.* 1216, 123602. <https://doi.org/10.1016/j.jchromb.2023.123602>.
- Yang, M., Luo, J., Li, Y., et al., 2020. Systems pharmacology-based research on the mechanism of Tusizi-Sangjisheng herb pair in the treatment of threatened abortion. *Biomed Res. Int.* 2020, 4748264. <https://doi.org/10.1155/2020/4748264>.
- Yang, S., Xu, H., Zhao, B., et al., 2016. The difference of chemical components and biological activities of the crude products and the salt-processed product from Semen Cuscutae. *Evid. Based Complement. Alternat. Med.* 2016, 8656740. <https://doi.org/10.1155/2016/8656740>.
- Yang, S., Xu, X., Xu, H., et al., 2017. Purification, characterization and biological effect of reversing the kidney-yang deficiency of polysaccharides from semen cuscutae. *Carbohydr. Polym.* 175, 249–256. <https://doi.org/10.1016/j.carbpol.2017.07.077>.
- Zhang, Y., Xiong, H., Xu, X., et al., 2018. Compounds identification in Semen Cuscutae by Ultra-High-Performance Liquid Chromatography (UPLCs) coupled to electrospray ionization mass spectrometry. *Molecules (Basel, Switzerland)* 23. <https://doi.org/10.3390/molecules23051199>.
- Zhou, H., Zheng, X., Wang, H., et al., 2022. Difference in network mechanism of Shoutaiwan and Juyuanjian in reversing pathology of decidua of spontaneous abortion patients: Based on “Uterine Collaterals Connecting Kidney” and “Fetal Collaterals Connecting Spleen” theory. *Chin. J. Exp. Tradit. Med. Formulae* 28, 186–200.
- Zhu, G.S., Tang, L.Y., Lv, D.L., et al., 2018. Total flavones of *Abelmoschus manihot* exhibits pro-angiogenic activity by activating the VEGF-A/VEGFR2-PI3K/Akt signaling axis. *Am. J. Chin. Med.* 46, 567–583. <https://doi.org/10.1142/s0192415x18500295>.